

## Cooperative adsorption of proteins onto lipid membranes

This article has been downloaded from IOPscience. Please scroll down to see the full text article.

2006 J. Phys.: Condens. Matter 18 S1257

(<http://iopscience.iop.org/0953-8984/18/28/S09>)

View [the table of contents for this issue](#), or go to the [journal homepage](#) for more

Download details:

IP Address: 129.252.86.83

The article was downloaded on 28/05/2010 at 12:20

Please note that [terms and conditions apply](#).

# Cooperative adsorption of proteins onto lipid membranes

Anne Hinderliter<sup>1</sup> and Sylvio May<sup>2</sup>

<sup>1</sup> Department of Pharmaceutical Sciences, North Dakota State University, Fargo, ND 58105, USA

<sup>2</sup> Department of Physics, North Dakota State University, Fargo, ND 58105, USA

Received 31 January 2006

Published 28 June 2006

Online at [stacks.iop.org/JPhysCM/18/S1257](http://stacks.iop.org/JPhysCM/18/S1257)

## Abstract

The adsorption of proteins onto a lipid membrane depends on and thus reflects the energetics of the underlying substrate. This is particularly relevant for mixed membranes that contain lipid species with different affinities for the adsorbed proteins. In this case, there is an intricate interplay between lateral membrane organization and the number of adsorbed proteins. Most importantly, proteins often tend to enhance the propensity of the lipid mixture to form clusters, domains, or to macroscopically phase separate. Sigmoidal binding isotherms are the typical signature of the corresponding cooperativity in protein adsorption. We discuss the underlying thermodynamic basis, and compare various theoretical binding models for protein adsorption onto mixed membranes. We also present experimental data for the adsorption of the C2A protein motif and analyse to what extent these data reflect cooperative binding.

## 1. Introduction

In all living cells, numerous proteins interact with biomembranes. Transmembrane proteins are firmly anchored by hydrophobic interactions to the hydrocarbon core of the host membrane. If the bilayer is in its fluid-like state, the transmembrane proteins are still able to laterally diffuse, allowing the cell to continuously reorganize the spatial protein distribution. Another class of membrane-associated proteins are peripheral proteins. These are located outside the lipid bilayer core, interacting with the host membrane through weak noncovalent bonds. The corresponding interaction energies of individual protein–lipid contacts do not largely exceed the thermal energy. Thus, peripheral proteins are in a dynamic relationship with the host membrane, being either membrane-adsorbed or floating in the aqueous solution. The notion of a dynamic equilibrium applies equally to peripheral proteins that interact with membrane lipids and with other, often integral, proteins. It also includes lipid-anchored (GPI-anchored) or acylated proteins such as Src and Ras.

The current interest in protein binding results from the need to understand how the organization of biomembranes and hence, cellular function, is affected and regulated by adsorbed proteins. Two examples illustrate this need: first, the lipid phosphatidylinositol

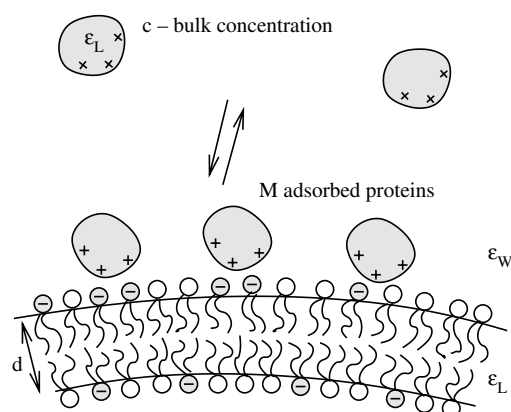


**Figure 1.** Schematic illustration of protein adsorption onto a lipid bilayer. Positively charged proteins (large shaded circles) are present in solution with concentration  $c$ ; the number of membrane-adsorbed proteins is  $M$ . The lipid bilayer is of thickness  $d$  and consists of charged and uncharged (zwitterionic) lipids. Generally, the lipid membrane may be bent, and the lipids belonging to different species may be distributed nonuniformly. We also note the largely different dielectric constants inside the macroions ( $\epsilon_L$ ) and in the aqueous environment ( $\epsilon_w$ ).

4,5-bisphosphate (PIP<sub>2</sub>) plays a key role in cell-signalling pathways and has various other regulatory functions [1]. Experimental evidence suggests that there are special proteins—among them the basic effector domain of myristoylated alanine-rich C kinase substrate (MARCKS)—that are able to sequester and, subsequently, release PIP<sub>2</sub>. Since it is a multivalently charged lipid, large forces must act to overcome the electrostatic repulsion between different PIP<sub>2</sub> molecules. Indeed, the effector region of MARCKS provides a cluster of 13 positive charges, enough to neutralize three PIP<sub>2</sub> molecules. Remarkably, no similar sequestration is observed [2] for monovalently charged lipids such as phosphatidylserine (PS). The second example is related to the protein synaptotagmin [3], which is involved in synaptic membrane fusion through its ability to bind lipid and calcium ions [4]. Synaptotagmins are composed of a trans-membrane sequence and two C2 domains, C2A and C2B, that differ in their acidic phospholipid specificities. Using a binding assay of the C2 protein motif on mixed membranes, it was previously shown that its presence can amplify the propensity of the lipid mixture to form PS-enriched domains [5, 6]. Moreover, small changes in the interaction energies between lipid components can strongly affect the degree of domain formation [6].

The binding of proteins onto a lipid membrane is schematically illustrated in figure 1. What makes the binding especially interesting is that the substrate—the membrane—is not a rigid, homogeneous surface (see Gray [7] for a discussion of this case) but can respond in various ways such as adjusting its local lipid composition [5, 8], bending [9], or even internalizing the adsorbed particle [10, 11]. Moreover, proteins often interact with each other, either directly or mediated through the membrane. Also, the adsorbing protein can undergo conformational changes as is often seen for amphipathic peptides that increase the amount of alpha-helical structure upon association with a membrane [12]. Another aspect is the different timescales pertaining to short and long term structural adjustments of the membrane–protein complex. For example, proteins that initially adsorb to the outer leaflet of a liposome may be able on a long timescale to enter the vesicle interior. Obviously, both cases require a different thermodynamic description. Finally, as protein adsorption is often driven by electrostatic interactions (or a combination of these and hydrophobic forces), electrostatic modelling is crucially important to understand the adsorption process.

In the following we analyse one particular aspect of protein binding onto lipid membranes both from a theoretical and experimental point of view. This aspect is the *cooperativity* in the binding process, including how that affects the binding isotherms and how it reflects the energetics of the underlying membrane. Section 2 presents several modelling approaches with some focus put on the use of different thermodynamic potentials to describe the binding. As protein binding onto membranes is often driven by electrostatic interactions, a short account of modelling electrostatic interactions in aqueous solution will be given. The final part in section 2 discusses an intriguing possibility characteristic to mixed fluid-like membranes, namely, membrane-mediated attractive interactions between adsorbed proteins. Section 3 is written from an experimental perspective. Our main objective here is to summarize an experimental approach in terms of the detection of cooperative protein binding onto lipid membranes.

## 2. Modelling approaches

### 2.1. Binding thermodynamics

We discuss the thermodynamic description of a binding process and the corresponding binding isotherm thereby focusing on how cooperative behaviour arises in protein binding and how this is reflected in the adsorption isotherms, particularly for mixed lipid membranes. A number of related approaches exist, such as an application of Cahn–Hilliard theory [13] or Monte Carlo simulations [14]. As in these studies we assume equilibrium adsorption (for a discussion of kinetic modelling see [15]).

Consider the situation that proteins of fixed chemical potential  $\mu$  bind onto a substrate (where at this point we do not need to specify the nature of the substrate). Denote the number of adsorbed proteins in thermal equilibrium by  $M$  and the maximal number by  $M_{\max}$ . A convenient way to calculate the adsorption isotherm (as in fact any thermodynamic quantity of the system) employs the *grand canonical partition function*

$$Q = \sum_{M_P=0}^{M_{\max}} e^{\mu M_P} \sum_i e^{-U_i(M_P)} \quad (1)$$

which adds all available states  $i$  (with corresponding internal energy  $U_i$ ) for all possible numbers  $M_P$  of adsorbed proteins, weighed according to the protein's chemical potential  $\mu$ . Note that in equation (1) and in the following we shall express all energies in terms of  $k_B T$ , where  $k_B$  is Boltzmann's constant and  $T$  is the absolute temperature. The grand canonical partition function  $Q$  is related to the corresponding *grand canonical potential*  $\Xi = -\ln Q = U - TS - \mu M$  (where  $U$  and  $S$  denote the internal energy and entropy, respectively) from which we obtain the *binding isotherm* through  $M = -(\partial \Xi / \partial \mu)_T$ . Note that this procedure is often most convenient and commonly used to calculate binding isotherms in biochemical/biophysical systems [16].

Perhaps the most simple case is the adsorption to independent and non-interacting adsorption sites, also referred to as Langmuir adsorption. In this case  $U_i = -M\epsilon$ , where the constant  $\epsilon > 0$  accounts for the gain in internal energy for each individually adsorbed protein. As is well known, the grand canonical partition sum evaluates to

$$Q = \sum_{M_P=0}^{M_{\max}} \frac{M_{\max}! e^{M_P(\epsilon+\mu)}}{M_P!(M_{\max} - M_P)!} = (1 + e^{\epsilon+\mu})^{M_{\max}} = (1 + cK)^{M_{\max}} \quad (2)$$

where in the latter equality we introduce the equilibrium constant  $K = e^\epsilon$  and we use the relation  $\mu = \ln c$  between the chemical potential  $\mu$  and the bulk concentration  $c$  of the proteins.

From equation (2) we find the Langmuir adsorption isotherm for the fractional membrane coverage  $\theta = M/M_{\max}$ , namely

$$\theta = \frac{cK}{1 + cK}. \quad (3)$$

At this point it is instructive to derive the Langmuir adsorption isotherm also through a somewhat different, less commonly used, method. To this end, we start with the free energy  $F = U - TS$  of the membrane as function of the fractional coverage  $\theta$ . In the absence of any protein–protein interactions we need to account only for the (ideal) demixing free energy and the gain in internal energy per protein, the latter being expressed by  $\epsilon$ . Thus

$$F(\theta)/M_{\max} = \theta \ln \theta + (1 - \theta) \ln(1 - \theta) - \epsilon \theta. \quad (4)$$

To account for the fixed chemical potential  $\mu$  of the proteins in solution we recall the grand canonical potential  $\Xi = F(\theta) - \mu M_{\max} \theta$ , which upon minimization with respect to  $\theta$  gives rise to  $\mu = d(F(\theta)/M_{\max})/d\theta$  and thus recovers equation (3).

Despite its approximations, the Langmuir adsorption model (bare or in conjunction with electrostatic free energy contributions [17]) is sometimes found to fit experimental adsorption data [18, 19]. More often, however, this will not be the case. One reason is that interactions among proteins are not taken into account. As will be pointed out below, such interactions do not only arise through direct protein–protein interactions, but they can also be mediated through the underlying membrane. A simple way to include attractive interactions between proteins is by employing the mean-field level (Bragg–Williams) approximation of a lattice-gas [20] which leads to the additional term  $\chi_P \theta(1 - \theta)$  on the rhs of equation (4). Here  $\chi_P > 0$  denotes the effective nearest-neighbour protein–protein attraction strength. Large  $\chi_P$  (that is, strong attraction) leads to lateral phase separation of the adsorbed protein layer (on the mean-field level  $\chi_P > 2$  is required). An interesting question is how relatively weak ( $0 < \chi_P < 2$ ) protein–protein attraction affects the adsorption isotherm. Such attraction renders the adsorption process *cooperative*, a typical signature of which is a *sigmoidal* shape of the adsorption isotherm (implying a point of inflection in  $\theta(c)$ ). Indeed, the Bragg–Williams model leads to the adsorption isotherm (graphically displayed in the left diagram of figure 2)

$$c \exp(\epsilon) = \frac{\theta}{1 - \theta} \exp[\chi_P(1 - 2\theta)] \quad (5)$$

which predicts an inflection point for solutions of the equation  $1 - 2\chi_P(1 - \theta)[1 - \chi_P\theta(1 - \theta)] = 0$ . As is seen in the inset to the left diagram of figure 2, the condition for the adsorption isotherm to have sigmoidal shape is  $\chi_P > 1/2$  (for a treatment beyond the mean-field level see [21]).

Both the Langmuir and Bragg–Williams isotherms describe the adsorption to localized adsorption sites. For proteins, especially for large ones that bind to many lipids at the same time, it is more appropriate to allow for a continuous adsorption surface instead. In this case, excluded volume effects generally tend to lower the number of adsorbed proteins [22, 23]. A simple model that conforms to the requirement of a continuous adsorption surface is the *van der Waals gas*, whose free energy can be written as

$$\frac{F}{M_{\max}} = \theta \left( \ln \frac{\theta}{1 - \theta} - 1 \right) - \epsilon \theta - \alpha \theta^2 \quad (6)$$

Here again,  $\epsilon$  denotes the gain in internal energy per individually adsorbed protein. The other constant,  $\alpha > 0$ , accounts for attractive interactions among the adsorbed proteins. Based on equation (6), one arrives at the adsorption isotherm [24, 25]

$$c \exp(\epsilon) = \frac{\theta}{1 - \theta} \exp \left[ \frac{\theta}{1 - \theta} - 2\alpha\theta \right] \quad (7)$$

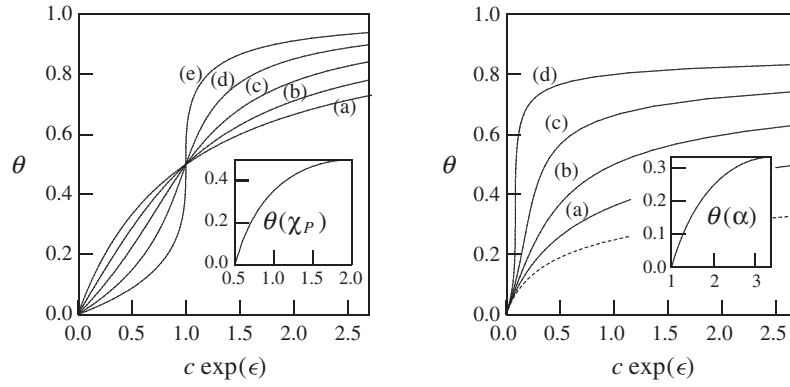


**Figure 2.** Adsorption isotherms  $\theta$  plotted as a function of  $c \exp(\epsilon)$ . Left diagram: Bragg–Williams model; see equation (5), with  $\chi_P = 0$  (curve (a)),  $\chi_P = 0.5$  (b),  $\chi_P = 1$  (c),  $\chi_P = 1.5$  (d), and  $\chi_P = 2$  (e). The inset shows the corresponding location of the inflection points, starting at  $\theta(\chi_P = 1/2) = 0$  extending to  $\theta(\chi_P = 2) = 1/2$ . Right diagram: van der Waals model; see equation (7), with  $\alpha = 0$  (a),  $\alpha = 1$  (b),  $\alpha = 2$  (c),  $\alpha = 3.375$  (d). The inset shows the corresponding location of the inflection points, starting at  $\theta(\alpha = 1) = 0$  extending to  $\theta(\alpha = 27/8) = 1/3$ . The broken line in the right diagram is the prediction of SPT; see equation (9).

which predicts a sigmoidal shape for  $\alpha > 1$  (extending up to  $\alpha = 27/8$ , above which the van der Waals gas is unstable (see the right diagram of figure 2 for plots of the adsorption isotherms and the inset for the location of the inflection points). We note that, for a hard sphere mixture in two dimensions, scaled particle theory (SPT) gives a more accurate expression of the free energy than the van der Waals model does. SPT predicts [26]

$$\frac{F}{M_{\max}} = \theta \left( \ln \frac{\theta}{1-\theta} - 1 \right) - \epsilon\theta + \frac{\theta^2}{1-\theta} \quad (8)$$

and thus a corresponding adsorption isotherm

$$c \exp(\epsilon) = \frac{\theta}{1-\theta} \exp \left[ \frac{3\theta}{1-\theta} + \left( \frac{\theta}{1-\theta} \right)^2 \right] \quad (9)$$

which is plotted in figure 2 (right diagram, broken line). Note that the SPT model only accounts for (the repulsive) excluded volume interactions but does not include any other protein–protein interaction. As can be seen from figure 2, SPT even more than the van der Waals model predicts reduced adsorption as compared to the Langmuir model. Both adsorption isotherms (see equations (7) and (9)) have been used in conjunction with a simple electrostatic interaction model to describe the binding of cytochrome C onto negatively charged membranes [27, 28]. It is also notable that the binding isotherms, given in equations (5), (7), and (9), are most conveniently derived using a model for the free energy  $F(\theta)$  of a membrane (instead of using the grand canonical potential  $\Xi(\mu)$ ).

The models presented so far account on different levels for excluded volume repulsion and direct protein–protein attraction. We emphasize that attractive interactions between the adsorbed particles induce cooperative behaviour (and, above a certain interaction strength the adsorption isotherm adopts a sigmoidal shape). The key mechanism is an increase in the probability of adsorbing proteins entailed by already adsorbed proteins. Models that lack this property are not cooperative. Consider, for example, the binding of a single protein to  $n$  lipids of a lipid species that is present in the membrane with composition (that is, mole fraction)  $\phi$ .

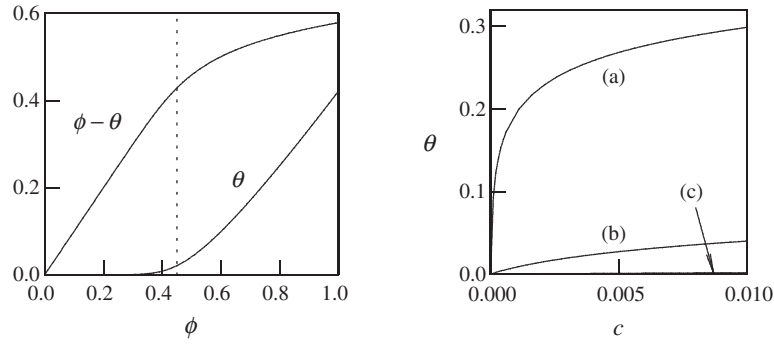


**Figure 3.** A model for binding of a single protein to  $n$  lipids. Left diagram: the coverage  $\theta$  and the free lipid fraction  $\phi - \theta$  as a function of membrane composition  $\phi$  for  $n = 10$ ,  $\epsilon = 0.8$  and  $c = 0.0034$ . The critical composition  $\phi_c = \exp(-\epsilon) = 0.45$  is marked by the vertical dashed line. Right diagram:  $\theta(c)$  for  $n = 10$ ,  $\epsilon = 0.8$ . The three different curves correspond to  $\phi = 0.8$  (a),  $\phi = 0.45$  (b), and  $\phi = 0.3$  (c).

Denoting again the protein coverage by  $\theta$  and the lipid–protein interaction per lipid by  $\epsilon$ , the adsorption isotherm  $\theta(c)$  fulfils the equation

$$e^{n\epsilon} c = \frac{\theta/n}{(\phi - \theta)^n}. \quad (10)$$

It is notable that  $\theta(\phi)$  exhibits a well-known kind of cooperative behaviour: for  $n \gg 1$  adsorption of particles sets in only above the well-determined critical composition [29]  $\phi_c = \exp(-\epsilon)$  as is shown for a specific example in the left diagram of figure 3. However, there is no sigmoidal behaviour in the binding isotherms  $\theta(c)$ , as can be seen in the right diagram of figure 3.

## 2.2. Electrostatic membrane–protein interactions

Adsorption of proteins onto charged lipid membranes is often driven (or enhanced [30, 31, 17]) by electrostatic interactions and can be modelled on the basis of Poisson–Boltzmann (PB) theory. A characteristic feature of many biologically occurring macroions, including lipid membranes and proteins, is their small dielectric constant  $\epsilon_L \approx 2\text{--}4$  as opposed to the large one of water, where  $\epsilon_W \approx 80$ . Hence, the dielectric constant  $\epsilon(\mathbf{r})$  undergoes large variations within any membrane–protein complex immersed in aqueous solution. Therefore, Poisson’s equation for the electrostatic potential  $\Phi(\mathbf{r})$  should be written as  $\nabla \epsilon \cdot \nabla \Phi + \epsilon \nabla^2 \Phi = -(\rho_f + \rho_m)/\epsilon_0$ , where  $\epsilon_0$  is the permittivity in vacuum. The local charge density,  $\rho_f + \rho_m$ , contains two contributions. The first,  $\rho_f$ , accounts for the fixed charges that are firmly attached to or reside within the macroion. The second,  $\rho_m = e(n_+ - n_-)$ , characterizes the mobile charges (monovalently charged co-ions and counter-ions of local concentrations  $n_+(\mathbf{r})$  and  $n_-(\mathbf{r})$ ) in the aqueous region ( $e$  denotes the elementary charge; generalization to higher valencies is straightforward [29]). The PB approach is a mean-field level description of the diffuse layer that surrounds each macroion; it predicts the Boltzmann distributions  $n_{\pm} = n_0 \exp(\mp \Psi)$  where  $\Psi = e\Phi/k_B T$  is the reduced potential (at room temperature  $\Psi = 1$  for  $\Phi = 25$  mV). Inserting the Boltzmann distributions into the Poisson equation, and defining the reduced dielectric constant  $\tilde{\epsilon}(\mathbf{r}) = \epsilon(\mathbf{r})/\epsilon_W$  in terms of that in water (where  $\epsilon_W \approx 80$ ), gives rise to the Poisson–

Boltzmann equation

$$\nabla \tilde{\epsilon} \cdot \nabla \Psi + \tilde{\epsilon} \nabla^2 \Psi = \begin{cases} \frac{1}{l_D^2} \sinh \Psi & \text{salt accessible regions} \\ \frac{-4\pi l_B}{e} \rho_f & \text{elsewhere.} \end{cases} \quad (11)$$

Here, the Debye length  $l_D = (8\pi n_0 l_B)^{-1/2}$  ( $l_D \approx 10$  Å in physiological 0.1 M salt solution) is expressed in terms of the Bjerrum length  $l_B = e^2/4\pi k_B T \epsilon_0 \epsilon_W$  ( $l_B \approx 7$  Å in water) and of the bulk ionic concentrations  $n_0 = n_{\pm}(\mathbf{r} \rightarrow \infty)$ . Note that the PB approach, being a mean-field theory, ignores interionic correlations. While this can be important for the interaction between like-charged macroions [32], it is much less significant for oppositely charged macroions (including protein adsorption onto an oppositely charged membrane).

Advanced numerical methods have evolved to solve equation (11) for atomistic representations of proteins and lipid membranes [33, 34], and a considerable number of macroions—proteins [35, 36], peptides [37], drugs [38], and sterols [39]—associated with lipid membranes have been investigated recently. An additional simplification should also be mentioned: the charged residues of biologically relevant macroions are typically located at the macroion's interface where  $\epsilon(\mathbf{r})$  changes rapidly from  $\epsilon_L$  and  $\epsilon_W$  (this is a manifestation of the high energy penalty to locate a single charge inside a body of low dielectric constant). It allows us to define a surface charge density  $\sigma$  and to treat the macroion's interior as uncharged. In fact, the interior of the macroions can entirely be ignored in PB theory as long as  $\epsilon_L l_D \ll \epsilon_W d$ , where  $d$  is the minimal lateral extension of the macroion (typically,  $d \approx 4$  nm for a lipid membrane,  $d \gtrsim 2$  nm for proteins,  $d \approx 2$  nm for DNA). With that, the PB equation can be written as  $l_D^2 \nabla^2 \Psi = \sinh \Psi$  and it needs to be solved only within the aqueous region (where  $\epsilon(\mathbf{r}) \equiv \epsilon_W$  and thus  $\tilde{\epsilon} \equiv 1$ ). Based on that equation, a large number of theoretical studies on the mutual electrostatic interaction between molecules of generic geometries have been performed in the past; see for example [40–43]. The use of generic geometries refers to the fact that typical charged biomolecules can be represented as planar surfaces (membranes), spheres (globular proteins), or cylinders (DNA or filaments). Also the case relevant to protein adsorption—plane–sphere geometry—has received some attention, as will be discussed below.

Generally, PB theory predicts an increase in counterion concentration in the vicinity of each macroion. In other words, the counter-ions are (partially) immobilized. Upon interaction of two oppositely charged macroions the respective counter-ions are released, which constitutes the main driving force for macroion association in aqueous solution. To illustrate this general notion, we consider a simple example, two planar surfaces (more detailed treatments of the planar geometry are available [44–46]), each of lateral area  $A$ , having opposite surface charge densities  $\sigma_{\pm} = \pm e/a$ , where  $a$  is the cross-sectional area per charge. The change in free energy  $f = Fa/A$  per surface charge upon association (starting from the fully separated state) is

$$f = \underbrace{\frac{q-1}{p}}_u + 2 \ln(p+q) - 3 \underbrace{\frac{q-1}{p}}_{-Ts} \quad (12)$$

where  $p = 2\pi l_B l_D/a$  and  $q = \sqrt{p^2 + 1}$ . The corresponding contributions arising from the energy stored in the electrostatic field ( $u$ ) and from the entropy of the mobile ions ( $-Ts$ ) are indicated in equation (12). As is easily verified, the entropic contribution is generally larger than the energetic one, and the ratio  $-Ts/u \geq 1$  increases with decreasing  $a$  (only in the limit  $a \rightarrow \infty$  do we have  $u = -Ts$ ). Geometries different from the planar one can somewhat modify this behaviour [47, 48].

Apart from a few simple geometries, it is not possible to analytically solve the PB equation. This includes the geometry of a sphere interacting with a planar surface which is



a reasonable first approximation of a single protein that adsorbs onto a flat membrane. Thus, numerical solutions are required. Indeed, there are a number of approaches (based on both the non-linear and linearized PB equation) to calculate double layer interaction energies for various geometries, including equal [49, 50] and unequal spheres [51, 47], and the plane–sphere geometry [52, 48]. As for the interaction between two planar surfaces, these studies show the dominating contribution of counterion release entropy for the plane–sphere geometry and identify regimes where analytical approximations (such as the Derjaguin or the linear superposition approximation) can be used.

Charged lipid membranes are almost always a mixture of uncharged (that is, zwitterionic) and charged lipids. Being in the fluid-like state, they have a demixing degree of freedom which may lead to the accumulation of charged lipids at a protein adsorption site. This lipid sequestration is schematically illustrated in figure 1. It can be taken into account within PB theory by a special condition for the local composition  $\eta$  at the membrane. Assuming ideal demixing of the lipids, this condition is given by [53, 8]

$$\eta = \frac{1}{1 + \frac{1-\phi}{\phi} \exp(\Psi_0 - \Psi)} \quad (13)$$

where  $\Psi_0 = -\ln(p + q)$  is the potential of the (homogeneously mixed and negatively charged) bare membrane. The approach of a positively charged protein will shift  $\Psi$  towards more positive values, thus increasing  $\eta$  above the bulk value  $\phi$ . Because of its generality, equation (13) can be applied to the interaction of mixed, charged membranes with any other macroion, including another membrane [54].

Another mechanism that affects the electrostatic contribution to the membrane–protein interaction energy is charge regulation [55, 56]. (Again, similar effects apply to other geometries such as a long cylinder adsorbed onto a membrane [57].) Here, the ionization state of titratable residues on the protein or on the membrane represents an additional degree of freedom which generally increases the interaction strength between these macroions. The corresponding pH-dependent gain in free energy can amount to several  $k_B T$  [55].

### 2.3. Membrane-mediated protein–protein interactions

There is currently a large interest in biomembrane domains (membrane rafts [58]), which results from a multitude of biological functions that has been shown to correlate with rafts. Models for the energetics of the complex *in vivo* systems and the crucial role of cholesterol have just started to emerge [59]. Interesting insights about the energetics of charged, mixed membranes can be gained already on a much simpler level. Consider for example a single planar membrane (in fact, one monolayer is sufficient). The above-mentioned Bragg–Williams model may be combined with the electrostatic free energy according to PB theory. Denoting the composition of the monolayer by  $\phi$  (mole fraction of charged lipids), the free energy per lipid,  $F/N$ , of the combined model reads

$$\frac{F}{N} = \phi \ln \phi + (1 - \phi) \ln(1 - \phi) + \chi \phi(1 - \phi) + 2\phi \ln(2\pi \phi l_B l_D / a) \quad (14)$$

where the last term is the high charge limit of equation (12) (with the replacement  $a \rightarrow a/\phi$ ). Note that  $\chi > 0$  only accounts for non-electrostatic, next-neighbour attraction. As discussed previously [60, 61], the lipid charges upshift the critical point of the membrane from  $\chi = 2$  to 3.7 (with critical compositions of  $\phi = 0.5$  and 0.63, respectively). A similar conclusion is reached based on the van der Waals model

$$\frac{F}{N} = \phi \left( \ln \frac{\phi}{1 - \phi} - 1 \right) - \alpha \phi^2 + 2\phi \ln(2\pi \phi l_B l_D / a) \quad (15)$$

where here again the last term is the electric double-layer free energy in the high charge limit. The van der Waals model leads to an upshift in the critical point from  $\alpha = 3.375$  to 5.895 (and corresponding critical compositions of  $\phi = 1/3$  and 0.446, respectively). These models, valid in the absence of adsorbed proteins, already show that the membrane energetics and lateral stability depend strongly on electrostatic interactions and should thus also be affected by the adsorption of oppositely charged proteins.

The electrostatic adsorption of proteins onto a mixed membrane opens an interesting possibility: proteins can be expected to locally sequester the lipid with high affinity for the protein. The result is a compositional difference  $\Delta\phi = \phi_P - \phi_L$  between the protein adsorption region ( $\phi_P$ ) and the bare membrane ( $\phi_L$ ). The magnitude of  $\Delta\phi$  depends not only on the difference in affinities of the two lipids for the protein but also on the number of adsorbed proteins, on the average membrane composition  $\phi$ , and (if present) on the degree of non-ideal mixing within the membrane. In terms of electrostatic protein adsorption onto a mixed anionic–zwitterionic membrane, the acidic lipid has high affinity and the zwitterionic lipid low affinity for the basic protein. The key point is the presence of non-ideal mixing within the membrane, namely, attractive lipid–lipid interactions as expressed by  $\chi > 0$ . It can be shown [61, 62] that these attractive interactions between the lipids in the membrane mediate effective interactions between the adsorbed proteins via

$$\chi_P \sim \chi (\Delta\phi)^2. \quad (16)$$

In other words, the protein–protein interaction parameter  $\chi_P$ , present in equation (5), can emerge through interactions within the membrane substrate; no direct protein–protein attraction is needed for the cooperative effects described in section 2 to arise. Similar considerations as for equation (5) apply for the other adsorption models we have presented (see equation (7) where  $\alpha$  plays a role similar to  $\chi_P$ ). The ability of proteins to induce domains in mixed membranes can thus be expected to depend on the interactions between the lipids. The combination of equations (5) and (16) suggests that cooperative behaviour in a protein binding isotherm  $\theta(c)$  may arise due to an increased propensity of the underlying lipid matrix to demix (corresponding to an increase in  $\chi$ ).

### 3. Remarks on experimental realization

As was mentioned in section 2, binding in experimental systems is commonly described by the grand canonical partition function  $Q$ . It is worthwhile to understand how experiments are carried out and how this relates to  $Q$ . In most binding experiments [5, 63–66], the concentration of the macromolecule (which here is the protein) is held constant and that of the ligand (here, the membrane) is varied. The grand canonical partition function  $Q$  is determined at fixed temperature, volume, and chemical potential conditions. This constraint holds for each experimental point, as with each addition of ligand, the volume and the chemical potential of both the free ligand, and free macromolecule changes. Because the added ligand is suspended in an aqueous solution, the volume  $V$  increases. This change in volume must, of course, be taken into account in the thermodynamic analysis of the adsorption data.

#### 3.1. Lipid accessibilities by proteins

The simple addition of a liposomal membrane, the ligand, to the system needs to be considered carefully because the liposome is a soft material that, dependent on the preparation, will have variable numbers of protein-accessible lipids. Liposomes may be formed in a variety of ways: multilamellar vesicles (MLVs) are stacked bilayers; they suffer from the disadvantage that, as they are formed upon vortexing hydrated lipid thin films, the distribution of sizes of liposomes

is unknown. MLVs also strongly scatter light, which is problematic when optical methods are used to follow ligand binding to macromolecules. Small unilamellar vesicles (SUVs), formed upon sonication of MLVs, are small in diameter and, thus, have high curvature. It is this high curvature that makes SUVs prone to fusion under various environmental conditions such as incubation at low temperatures. In contrast, large unilamellar vesicles (LUVs) are formed upon extrusion of MLVs through pores of defined sizes and, therefore, suffer neither from an undefined size distribution nor from having a high propensity to fuse.

Beyond the problems of simply adding membrane ligand reproducibly, the challenge of determining the concentration of specific lipids within the liposome also arises. This is as the *effective concentration* of a lipid changes with the composition of the other lipids present in the liposome. What we mean by effective concentration is that the affinity of the macromolecule for a ligand is described by the *activity* of the ligand. The activity of the free ligand is directly proportional to its chemical potential. If a lipid mixed randomly with the other components of a membrane, its activity would equal its physical concentration within the membrane.

A caveat is that proteins in the aqueous solution can only interact with the lipids in the outer leaflet of newly added liposomes. Thus, the lipids in the inner leaflet of an intact liposome do not contribute to the initial binding process. However, structural defects such as membrane pores can induce fast lipid flip-flop and thus induce asymmetric lipid distributions of mixed, protein-decorated liposomes. Even in the absence of structural defects, slow flip-flop will be directed towards re-establishing thermal equilibrium to compensate for changes in the chemical potentials of the lipids upon protein binding. As the lipid's chemical activity is influenced by its neighbours, the local perturbation induced by protein binding will have consequences communicated to the opposite leaflet. The difference in chemical potentials will be sensed and equilibrated until they again become equal.

How do we express the extent of non-random mixing and ascertain the effective concentration of the lipids? In a binary lipid mixture, the deviation from ideal mixing can be expressed by the non-ideality parameter  $\chi = z[\omega_{12} - (\omega_{11} + \omega_{22})/2]$  ( $z$  is the coordination number underlying the lattice-gas model). Note that, while the individual lipid–lipid interaction energies,  $\omega_{11}$ ,  $\omega_{22}$ , and  $\omega_{12}$ , between lipids of species ‘1’ and ‘2’ can be large,  $\chi$  itself is usually small. Hence, it is the net *difference* in the interaction energies between like and unlike lipids that readily alters the effective concentration of each lipid. If the net difference in interaction energies was large, the system would macroscopically phase separate (this is predicted to occur for  $\chi > 2$  on the mean-field level). At the extreme of complete phase separation, the effective lipid concentration would revert to the physical concentration of lipid in the bilayer if each of the two coexisting phases is sufficiently dilute with respect to one lipid species.

### 3.2. Sensitivity of lateral membrane organization to protein adsorption

A protein may remodel a membrane surface to enhance favourable contacts with the lipid species for which it has high affinity. The membrane itself can through nonideal mixing of the lipid components lead to both enhanced and suppressed protein binding. As an instructive example, consider a protein comprised of a membrane-binding surface which contains two different parts: one with positively charged and one with neutral residues. Obviously, such a hypothetical protein would preferentially adsorb to a domain boundary of a mixed anionic–zwitterionic lipid membrane [67]. Let us consider two different scenarios: if the lipid–lipid interaction energies are small, then, upon association of the protein with the membrane surface, the favourable contacts of protein with different membrane lipids will create an enriched acidic lipid surface under the cationic portion of the protein and a zwitterionic lipid surface under the neutral protein surface. This leads to an enhancement of the membrane to form (protein-

decorated) lipid domains. On the other hand, if the lipid–lipid interaction energies are large, then the membrane will macroscopically phase separate. In this case, protein binding will initially fill all pre-existing binding sites on the phase domain boundaries. Further adsorption then may partially occur onto the bulk phases but will ultimately tend to create new phase boundaries, thus diminishing the size of the membrane domains. Here, the protein acts like a surfactant [68] that dissolves the membrane domains. The resulting lateral membrane structure is the net result of both optimizing protein–lipid contacts as well lipid–lipid interactions. Our example shows that proteins do not necessarily always act towards segregating lipids.

### 3.3. Recapitulation of an experimental approach

To ascertain the magnitude of protein–membrane interactions, commonly, experiments were based on a procedure in which lipid vesicles with corresponding lipid concentration  $N_t/V$  are titrated into an aqueous solution containing protein of concentration  $[M_t] = M_t/V$  (where  $V$  is the volume of the aqueous solution). What is measured in experiment [65] is a signal  $S$ , being proportional to the number  $M$  of membrane-bound proteins. We write  $\theta_E = M/M_t = S/S_{\max}$ , where  $S_{\max}$  would be the experimental signal if all proteins were membrane-adsorbed. The protein coverage  $\theta = M/M_{\max}$  on the membrane reflects the actual versus maximal number of membrane-adsorbed proteins. We assume that  $M_{\max} = N_t/(2m)$ , where  $m$  is the number of lipids within a single protein adsorption site; the additional factor of 2 accounts for 50% of the lipids in the inner leaflet of the added liposomes not being accessible to the proteins. Finally we note that  $cV = M_t - M$ , where  $c$  is the actual concentration of unbound proteins. From these relations we arrive at

$$\theta = 2m \frac{S}{S_{\max}} \frac{[M_t]}{[N_t]}, \quad c = [M_t] \left( 1 - \frac{S}{S_{\max}} \right) \quad (17)$$

which allows us to convert any experimental data set  $S([N_t])$  to  $\theta(c)$ , given that  $m$ ,  $S_{\max}$ , and  $[M_t]$  are known. Of course, the inverse relations,  $S = S(\theta, c)$  and  $[N_t] = [N_t](\theta, c)$ , can also be derived. Based on equations (17) it is notable that the Langmuir adsorption isotherm,  $\theta(c) = cK/(1 + cK)$ , converts again into a Langmuir adsorption isotherm  $\theta_E = [M_f]K/(1 + [M_f]K)$  if plotted as a function of the number of unoccupied membrane adsorption sites,  $[M_f] = M_f/V = (M_{\max} - M)/V$ . However, other binding models (see figures 2 and 3) generally lead to different functional forms of  $\theta(c)$  and  $\theta_E([M_f])$ . In particular, sigmoidal behaviour (that is, the appearance of a point of inflection) in  $\theta(c)$  does not translate to sigmoidal behaviour in  $\theta_E([M_f])$ . This is an important aspect of analysing binding isotherms.

To see the current challenges in measuring cooperative behaviour in protein binding for biologically relevant lipid mixtures, we present two experimentally derived binding isotherms  $S([N_t])$  for the C2A domain of the protein synaptotagmin; see figure 4. The two data sets refer to two different lipid compositions of a 1-palmitoyl-2-oleoyl-*sn*-glycerol-3-phosphocholine, 1-palmitoyl-2-oleoyl-*sn*-glycerol-3-phosphoserine, and diacylglycerol (POPC/POPS/DAG) mixture. The inset displays the same two data sets converted to  $\theta(c)$  according equation (17). As the underlying model, the van der Waals gas (see equation (7)) was used. Three parameters, namely  $K$ ,  $\alpha$  and  $S_{\max}$ , result from the fit. In both cases we find  $\alpha > 1$ , which we recall from figure 2 as the condition for the binding isotherms to exhibit sigmoidal behaviour. The sigmoidal shape of  $\theta(c)$  is indeed evident from the fitted curves in the inset of figure 4 (and a similar conclusion is valid if instead of the van der Waals gas model, equation (5) is used). Most notably, as the protein–protein attraction strength  $\alpha$  depends on the membrane composition, it must represent membrane-mediated effects. At present, however, there are substantial concerns whether the fit of the experimental data sets by a sigmoidal curve indeed reflects cooperative binding. First of all, the scattering—particularly for large  $c$ —in the experimental data is

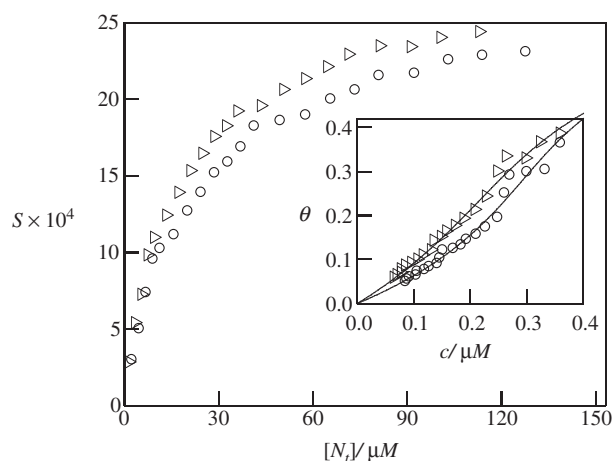


**Figure 4.** The raw experimental data with corresponding fluorescence signal  $S$  as a function of the total added lipid concentration  $[N_t]$ ; the different symbols correspond to C2A adsorbed on a membrane of composition POPC/POPS/DAG: 0.64/0.16/0.2 (○) and POPC/POPS/DAG: 0.72/0.18/0.1 (▷). Note that the total protein concentration used in the experiments was  $[M_t] = 0.45 \mu\text{M}$ . The inset replots the data as  $\theta(c)$  and shows fits to the van der Waals gas model (see equation (7)). The fitting parameters are  $K = 0.54$ ,  $\alpha = 2.3$  (○) and  $K = 0.79$ ,  $\alpha = 1.9$  (▷). The number of lipids per protein adsorption site was assumed to be  $m = 10$ .

substantially. A reduction of this scattering at large  $c$  would require us to measure  $S([N_t])$  more accurately for small  $[N_t]$ , which is difficult to achieve experimentally. Second, the fitted curves for  $\theta(c)$  also depend on  $m$ , the number of lipids per protein adsorption site. By comparing the steric size of the adsorbed C2A segment with the cross-sectional area per lipid ( $\approx 70 \text{ \AA}^2$ ), this number should be of the order of  $m \approx 10$  (this value is also used in figure 4). Yet, a more accurate knowledge of  $m$  would be required for a more reliable estimate of  $\alpha$  (or, similarly,  $\chi$ ). Finally, there are mechanisms not accounted for in the derivation of the binding isotherms that, at present, cannot be excluded to contribute to the shape of the binding isotherms. Among those are structural defects in the liposomes that affect the number of protein-accessible lipids (those would alter  $m$ ), or aggregation processes, including protein-mediated aggregation, of the liposomes in solution. These considerations suggest that we are presently not able to unequivocally detect cooperativity in protein binding isotherms onto fluid lipid membranes and to relate that to the energetics of the underlying substrate. However, upon refining the present or developing alternative binding assays, progress in probing membrane energetics through protein binding is likely.

#### 4. Summary and conclusions

We have suggested methods to model and analyse the cooperativity of protein binding onto (fluid-like) lipid membranes. A minimal protein–protein interaction strength was calculated above which the binding isotherms are expected to exhibit sigmoidal behaviour. We argued that interactions between proteins can also be mediated by the underlying membrane. In this case, the shape of the binding isotherm reflects physical membrane properties such as attractive lipid–lipid interactions and a corresponding tendency to form domains or to macroscopically phase separate. We also discussed an experimental approach that suggests cooperativity but is not yet conclusive enough to reliably quantify the cooperativity strength.

## Acknowledgments

This work was supported through ND EPSCoR by grant No. EPS-0132289 (SM) and, in part, by grant GM64443 (AH) from the National Institute of Health. AH also thanks the donors of the Petroleum Research Fund of the American Chemical Society for support. SM acknowledges discussions with Avinoam Ben-Shaul and Emmanuel Mbamala.

## References

- [1] McLaughlin S, Wang J, Gambhir A and Murray D 2002 *Annu. Rev. Biophys. Biomol. Struct.* **31** 151
- [2] Golebiewska U, Gambhir A A, Hangyas-Mihalyné G, Zaitseva I, Rädler J and McLaughlin S 2006 *Biophys. J. preprint* doi:10.1529/biophysj.106.081562
- [3] Yoshihara M and Montana E S 2004 *Neuroscientist* **10** 566
- [4] Sudhof T C 2004 *Annu. Rev. Neurosci.* **27** 509
- [5] Hinderliter A, Almeida P F F, Creutz C E and Biltonen R L 2001 *Biochemistry* **40** 4181
- [6] Hinderliter A, Biltonen R L and Almeida P F F 2004 *Biochemistry* **43** 7102
- [7] Gray J J 2004 *Curr. Opin. Struct. Biol.* **14** 110
- [8] May S, Harries D and Ben-Shaul A 2000 *Biophys. J.* **79** 1747
- [9] Hurley J H and Wendland B 2002 *Cell* **111** 143
- [10] Domanov Y A, Molotkovsky J G and Gorbenko G G P 2005 *Biochim. Biophys. Acta* **1716** 49
- [11] Harries D, May S and Ben-Shaul A 2002 *Colloids Interfaces A* **208** 41
- [12] White S H and Wimley W C 1999 *Annu. Rev. Biophys. Biomol. Struct.* **28** 319
- [13] Schiller P, Mögel H J, Wahab M and Reimer U 2002 *J. Phys. Chem. B* **106** 12323
- [14] Tzliil S and Ben-Shaul A 2005 *Biophys. J.* **89** 2972
- [15] Minton A P 2001 *Biophys. J.* **80** 1641
- [16] Ben-Naim A 2001 *Cooperativity and Regulation in Biochemical Processes* (Berlin: Springer)
- [17] Gómez C M, Codoñer A, Campos A and Abad C 2000 *Int. J. Biol. Macromol.* **27** 291
- [18] Cutsforth G A, Koppaka V, Krishnaswamy S, Wu J R, Mann K G and Lentz B R 1996 *Biophys. J.* **70** 2938
- [19] Retzinger G S, Meredith S C, Lau S H, Kaiser E T and Kézdy F J 1985 *Anal. Biochem.* **150** 131
- [20] Hill T L 1960 *Introduction to Statistical Thermodynamics* (New York: Addison-Wesley)
- [21] Aranovich G L, Erickson J S and Donohue M D 2004 *J. Chem. Phys.* **120** 5208
- [22] Chatelier R C and Minton A P 1996 *Biophys. J.* **71** 2367
- [23] Minton A P 2000 *Biophys. Chem.* **86** 239
- [24] Hill T L 1947 *J. Chem. Phys.* **14** 441
- [25] Heimburg T and Marsh D 1996 *Biological Membranes. A Molecular Perspective from Computation and Experiment* ed K M Merz Jr and B Roux (Boston, MA: Birkhäuser) pp 405–62
- [26] Rosenfeld Y 1990 *Phys. Rev. A* **42** 5978
- [27] Heimburg T, Angerstein B and Marsh D 1999 *Biophys. J.* **76** 2575
- [28] Heimburg T and Marsh D 1995 *Biophys. J.* **68** 536
- [29] Evans D F and Wennerström H 1994 *The Colloidal Domain, Where Physics, Chemistry, and Biology Meet* 2nd edn (New York: VCH)
- [30] Pedersen T B, Sabra M C, Frokjaer S, Mouritsen O G and Jorgensen K 2001 *Int. J. Pharm.* **214** 77
- [31] Pedersen T B, Sabra M C, Frokjaer S, Mouritsen O G and Jorgensen K 2001 *Chem. Phys. Lipids* **113** 83
- [32] Grosberg A Y, Nguyen T T and Shklovskii B I 2002 *Rev. Mod. Phys.* **74** 329
- [33] Sitkoff D, Sharp K and Honig B 1994 *J. Phys. Chem.* **98** 1978
- [34] Nielsen J E, Andersen K V, Honig B, Hooft R W, Klebe G, Vriend G and Wade R C 1999 *Protein Eng.* **12** 657
- [35] Ben-Tal N, Honig B, Peitzsch R M, Denisov G and McLaughlin S 1996 *Biophys. J.* **71** 561
- [36] Ben-Tal N, Honig B, Miller C and McLaughlin S 1997 *Biophys. J.* **73** 1717
- [37] Wang J Y, Gambhir A, McLaughlin S and Murray D 2004 *Biophys. J.* **86** 1969
- [38] Kessel A, Musafia B and Ben-Tal N 2001 *Biophys. J.* **80** 2536
- [39] Kessel A, Ben-Tal N and May S 2001 *Biophys. J.* **81** 643
- [40] Sens P and Joanny J F 2000 *Phys. Rev. Lett.* **84** 4862
- [41] Harries D 1998 *Langmuir* **14** 3149
- [42] Menes R, Pincus P, Pittman R and Dan N 1998 *Europhys. Lett.* **44** 393
- [43] Sader J E and Chan D Y C 1999 *J. Colloid Interface Sci.* **218** 423
- [44] Lau A W C and Pincus P 1999 *Eur. Phys. J. B* **10** 175
- [45] Meier-Koll A A, Fleck C C and von Grünberg H H 2004 *J. Phys.: Condens. Matter* **16** 6041



- [46] Safran S A 2005 *Europhys. Lett.* **69** 826
- [47] Palkar S A and Lenhoff A M 1994 *J. Colloid Interface Sci.* **165** 177
- [48] Roth C M, Sader J E and Lenhoff A M 1998 *J. Colloid Interface Sci.* **203** 218
- [49] Carnie S L and Chan D Y C 1993 *J. Colloid Interface Sci.* **155** 297
- [50] Carnie S L, Chan D Y C and Stankovich J 1994 *J. Colloid Interface Sci.* **165** 116
- [51] Stankovich J and Carnie S L 1996 *Langmuir* **12** 1453
- [52] Warszynski P and Adamczyk Z 1997 *J. Colloid Interface Sci.* **187** 283
- [53] Harries D, May S, Gelbart W M and Ben-Shaul A 1998 *Biophys. J.* **75** 159
- [54] Russ C, Heimburg T and von Grünberg H H 2003 *Biophys. J.* **84** 3730
- [55] Lund M, Akesson T and Jönsson B 2005 *Langmuir* **21** 8385
- [56] Biesheuvel P M, van der Veen M and Norde W 2005 *J. Phys. Chem. B* **109** 4172
- [57] Fleck C, Netz R R and von Grünberg H H 2002 *Biophys. J.* **82** 76
- [58] Simons K and Ikonen E 1997 *Nature* **387** 569
- [59] Simons K and Vaz W L C 2004 *Annu. Rev. Biophys. Biomol. Struct.* **33** 269
- [60] Gelbart W M and Bruinsma R 1997 *Phys. Rev. E* **55** 831
- [61] May S, Harries D and Ben-Shaul A 2002 *Phys. Rev. Lett.* **89** 268102
- [62] Mbamala E C, Ben-Shaul A and May S 2005 *Biophys. J.* **88** 1702
- [63] Silvius J R and l'Heureux F 1994 *Biochemistry* **33** 3014
- [64] Srivastava A, Wang J, Majumder R, Rezaie A R, Stenflo J, Esmon C T and Lentz B R 2002 *J. Biol. Chem.* **277** 1855
- [65] Almeida P F, Sohma H, Rasch K A, Wieser C M and Hinderliter A 2005 *Biochemistry* **44** 10905
- [66] Rusu L, Gambhir A, McLaughlin S and Rädler J 2004 *Biophys. J.* **87** 1044
- [67] McConnell H M and Vrljic M 2003 *Annu. Rev. Biophys. Biomol. Struct.* **32** 469
- [68] Puech P H, Borghi N, Karatekin E and Brochard-Wyart F 2003 *Phys. Rev. Lett.* **90** 128304